UNITED NATIONS UNIVERSITY
UNU-GTP
Geothermal Training Programme

Orkustofnun, Grensasvegur 9,
IS-108 Reykjavik, Iceland

Reports 2014
Number 18

THERMODYNAMIC AND THERMOECONOMIC OPTIMIZATION OF A GEOTHERMAL POWER PLANT IN SICHUAN, CHINA

Luo Chao
GuangZhou Institute of Energy Conversion,
Chinese Academy of Sciences,
No. 2 Nengyuan Rd. Wushan, Tianhe District,
Guangzhou
CHINA
luochao@ms.giec.ac.cn

ABSTRACT

This report presents intermediate- and high-temperature geothermal fields distributed in China. Sichuan geothermal area has been selected for a new power plant in the near future, based on governmental policy and energy company demand. Five types of geothermal power systems are designed and presented for it. Using the EES and Scilab software, comparison and optimization of these power systems are analysed, taking into account thermodynamic and thermoeconomic laws. The results show that, for this geothermal system, a binary system is better than other systems. The optimum capacity of the binary system is 3506 kW and 3773 kW for the Tuo-Bei and Yu-Lingong geothermal fields, respectively. The power production cost is 0.04 US$/kWh for the binary system and the payback period is about 6 years. The thermodynamic and thermoeconomic optimization are determined by using basic data for the future power plant design in the Sichuan geothermal area.

1. INTRODUCTION

1.1 Objective and background

A geothermal power plant is different from a thermal power plant. The capacity of a geothermal power plant is not as easy to identify, compared with a thermal power plant as different capacity corresponds to different design criteria. In China, urban populations are provided with their electricity requirements, but rural areas need guaranteed electricity for socio-economic development. Fortunately, intermediate- to low-temperature geothermal resources are located in proximity to rural areas that are without access to grid electricity. Small-scale geothermal power plants can support electricity demand as well as create employment opportunities for the rural public. Existing geothermal power plants in China were built in the 1970s, their former designers and constructors have either retired or died. Recently, many big corporations have wanted to invest in geothermal power projects, during the "Twelfth Five-Year Plan", because of energy shortages and the government inspired energy policy in China.

The object of this paper is to design different types of geothermal power plants and optimize them, based on the geothermal fields in Sichuan, China.

1.2 Comparison of power plants that utilize renewable energy

Electrical energy can be generated from various sources, through conventional sources such as nuclear, coal, diesel, etc., and via renewable sources, such as geothermal, wind, solar energy, etc. One of the greatest problems in using renewable energy sources is the great variability in the energy level, both in the short and long term. Geothermal energy is highly desirable because the source is not dependent on weather conditions, so it is among the most stable renewable energy sources. Geothermal energy has proven to be reliable, clean, and safe; therefore, it is increasingly explored for power production, heating and cooling. Geothermal energy produces electricity with minimal environmental impacts. Table 1 gives the energy and investment costs for electric energy production from renewables (Valdimarsson, 2014).

TABLE 1: Energy and investment costs for electric energy production from renewables

	Current energy cost (US¢/kWh)	**Potential future energy cost (US¢/kWh)**	**Turnkey investment cost (US$/kW)**
Biomass	5 - 15	4 – 10	900 - 3000
Geothermal	2 - 10	1 – 8	800 - 3000
Wind	5 - 13	3 – 10	1100 - 1700
Solar (photovoltaic)	25 - 125	5 – 25	5000 - 10000
Solar (thermal electricity)	12 - 18	4 – 10	3000 - 4000
Tidal	8 – 15	8 – 15	1700 – 2500

1.3 Overview

The work in this study is primarily concerned with a geothermal energy utilization performance analysis and feasibility research. Section 2 presents intermediate- to high-temperature geothermal resources in China. Sections 3 and 4 concentrate on thermodynamic and thermoeconomic optimization, with Section 3 discussing the thermodynamic model of single-flash, double-flash, binary and flash-binary power systems, and the optimum value of turbine work and pressure, while Section 4 discusses the cost and thermoeconomic analysis of a binary system. Finally, a sensitivity analysis of geothermal temperature and flow rate are discussed. Finally, Section 5 presents the conclusions of this report.

2. GEOTHERMAL RESOURCE ASSESSMENT IN CHINA

2.1 Potential geothermal fields in China

In China, high-temperature geothermal resources are mainly distributed in South Tibet, West Sichuan, and West Yunnan; while intermediate-temperature geothermal resources are mainly distributed along the coastal areas of southeast China, including Guangdong, Hainan, Jiangxi, Hunan and Fujian. Figure 1 shows the main geothermal fields in China. The intermediate-temperature systems are, as expected, water-dominated. According to Wang and Ma (2005), the potential capacity of the geothermal resources for electrical production is about 8000 MW.

In Chaozhou, Guangdong province, the geothermal temperature is 104°C at 227 m; in Baoting, Hainan province, the geothermal temperature is 90°C at 168 m; in Sichuan, Jiangxi province, the geothermal temperature is 87.9°C at 520 m; in Ningxiang, Hunan province, the geothermal temperature is 102°C at 616 m; in Zhangzhou, Fujian province, the geothermal temperature is 121.5°C at 91 m. Table 2 gives the data on intermediate- to high-temperature (>120°C) geothermal fields in China (Lin and Liu, 2013; Wang and Ma, 2005).

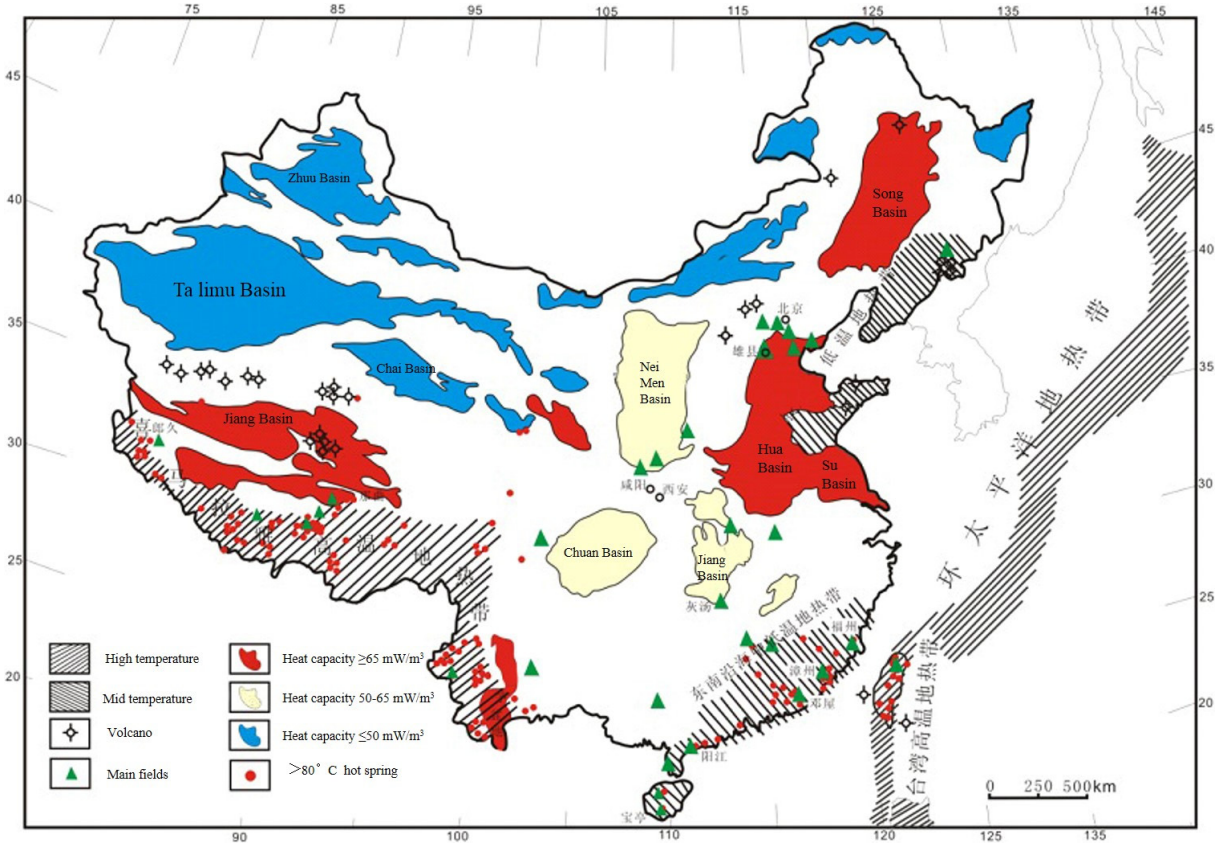

FIGURE 1: Geothermal fields in China

TABLE 2: Geothermal fields in China with intermediate to high temperatures

	Province		Name of field	Geothermal water (artesian flow)			Estimated reservoir data				Cooling water
				T (°C)	Flow rate (kg/s)	TDS (g/l)	T (°C)	Flow rate (kg/s)	Enthalpy (kJ/kg)	Gas mass fraction (%)	
1	Guang-dong	1	Yang-jiang	97	16.4	3	150-170	20-50	800	1	Y
		2	Deng-wu	87	4.5	0.33	135-160	100		0	Y
		3	Feng-liang	92	10.9	0.45	135-160	100		0	Y
		4	Chaozhou donghu	82	1	1.12	140			0	N
		5	Heping reshui	89	11.3	0.38	135			0	N
2	Tibet	6	Yang-bajing				141-172	70-100	1090	12-15	Y
		7	Yang-yi				188	70-80	1040	10-13	Y
		8	Na-qu					30-50			Y
		9	Lang-jiu				166	30-50	950	10-12	N
		10	Ta-ge-jia				189				N
		11	Cha-bu				228				N
		12	Bu-xiong-Lang-ji				245				N
3	Fujian	13	Fu-zhou	97	113	0.2-0.5	150-200	100-150	1050	8-10	N
		14	Zhang-zhou	105	87.8	9.1	130-170	80-100	950	5-6	Y
		15	Gui-an	90	23.3	0.37	143	50-80		0	Y
		16	Hua-an	93	115	0.25	120	80-150		0	Y
		17	Xia-men	91	50-70	14	130-170	50-100		0	Y
		18	San-ming				150			0	Y
		19	Quan-zhou				150			5	Y
4	Sichuan	20	Tuo-bei	96		2	170	20-50		0	Y
		21	Yu-lingong	92-100	5	1	180	20-50	800-1000	5-8	Y
		22	Ba-tang	80-100	3	0.7	250	20-50	900-1200	5-8	Y
		23	Li-tang	87			210	20-50	800-1000	5-8	Y

	Province		Name of field	Geothermal water (artesian flow)			Estimated reservoir data				Cooling water
				T (ºC)	Flow rate (kg/s)	TDS (g/l)	T (ºC)	Flow rate (kg/s)	Enthalpy (kJ/kg)	Gas mass fraction (%)	
5	Yunnan	24	Teng-chong	98	30-50	0.7-1.5	170-230	50-80		10-14	Y
		25	Rui-li	100	3-10	1	205	20-30		10-14	Y
		26	Yun-xian	100	30-50	0.5	180-210	50-80		10-14	Y
		27	Longlin bazhangla	100	9.01	0.71	210	20-40		10	Y
6	Hainan	28	Guan-tang	70-90			>150	30-60		0	Y
		29	Qi-xian-ting	93			>150	50-80		0	Y
		30	Lan-yang	93			>150	50-80		0	N
7	Hunan	31	Ning-xiang	90.5		<0.4	>120	80		0	Y
		32	Ru-cheng	92.5		0.658	>120	30		0	Y
8	Xinjiang	33	Hu zhu				100	10-20		0	N
		34	Tian shan				180	10-20		0	N

2.2 Weather conditions in Sichuan

Sichuan geothermal area is near Tibet; with intermediate- to high-temperature geothermal fields distributed in the west part of Sichuan. Because of governmental and energy corporation interests and policy, a new geothermal power plant may be built in the Sichuan province.

Weather data is taken from 2005. The data were recorded at 1 hour intervals. There are 7 hours missing from the dataset, so the data were extrapolated to 8760 hours. The data give the dry bulb temperature and relative humidity. The wet bulb temperature is then calculated for all valid data points. The dry and wet bulb temperatures from Jan 1st to Dec 31st are given in Figure 2.

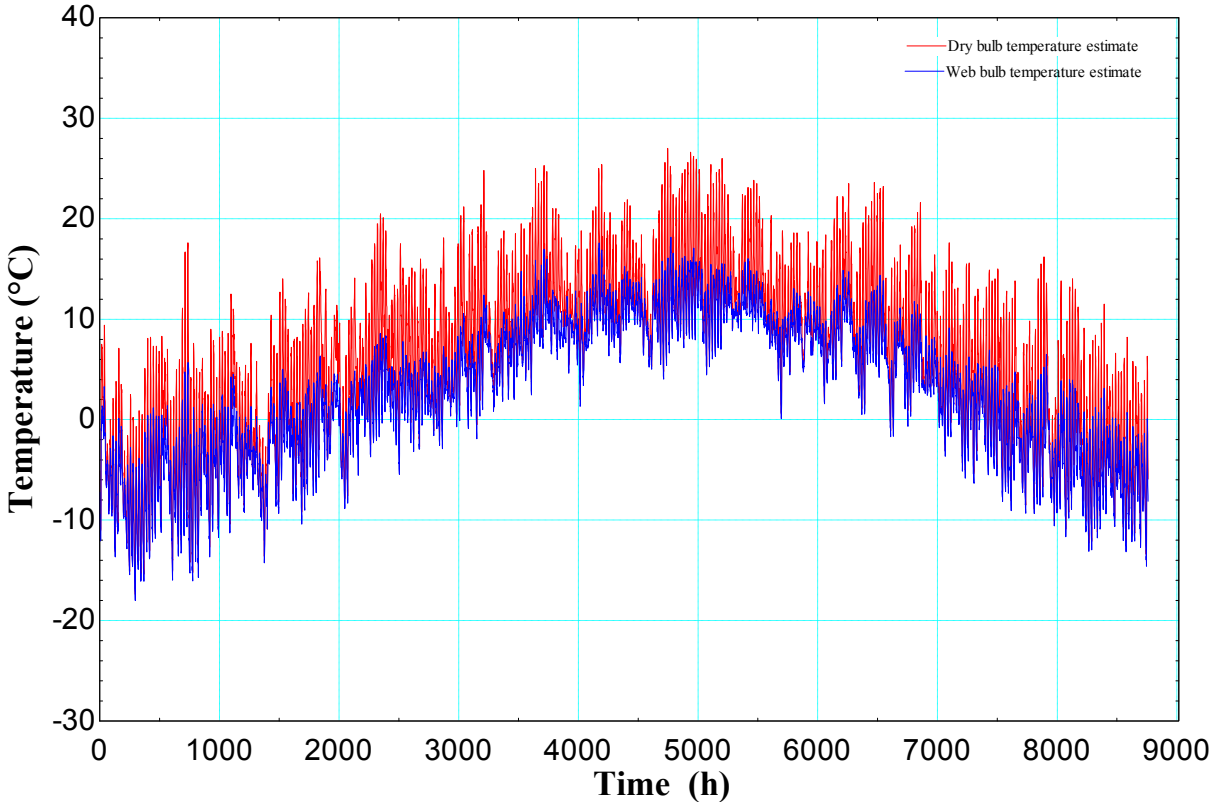

FIGURE 2: Dry bulb and wet bulb temperatures

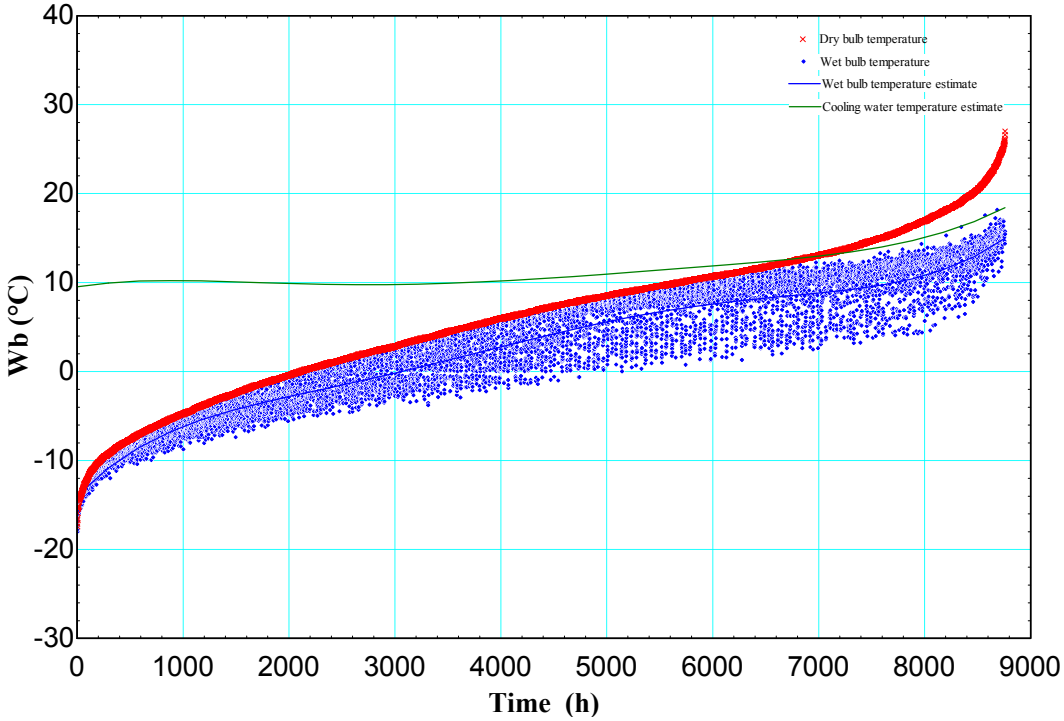

FIGURE 3: Cooling water temperature estimate

The duration curves for dry and wet bulb as well as estimated cooling water temperature are shown in Figure 3. The cooling water temperature is assumed to be 4°C higher than the wet bulb temperature at the hottest day. This temperature is assumed to be 10°C when the wet bulb temperature has fallen down to 0°C. The minimum cooling water temperature is assumed 10°C. A cooling water temperature of 15°C is selected in this paper for the design point (green line). The dry bulb temperatures are listed from the lowest to the highest.

Of the Sichuan geothermal fields, Tuo-bei and Yu-lingong were selected; non-condensed gas exists in the Yu-lingong geothermal field. In this report, single-flash, double-flash, binary and flash-binary power systems are designed for Tuo-bei field, and a gas-vapour-liquid binary system for Yu-lingong field. The assumptions for the geothermal system and technical characteristics of the plant systems are shown in Table 3.

TABLE 3: Parameters and boundary conditions of the power plant models for the Sichuan fields

	Parameter		Unit	Value
Geothermal reservoir	Tuo-bei	Temperature of reservoir	°C	170
		Mass flow rate	kg/s	50
		Gas mass fraction	%	0
	Yu-lingong	Temperature of reservoir	°C	180
		Gas mass fraction	%	8
		Mass flow rate	kg/s	50
Power plant system	Cooling water temperature		°C	15
	Temperature difference of cooling water		°C	10
	Turbine isentropic efficiency		%	80
	Pump isentropic efficiency		%	75
	Vaporizer heat transfer coefficient		kW/(m^2.°C)	1.1
	Preheater heat transfer coefficient		kW/(m^2.°C)	0.7
	Recuperator heat transfer coefficient		kW/(m^2.°C)	0.7
	Condenser heat transfer coefficient		kW/(m^2.°C)	1

2.3 Literature review

There are three main kinds of commercialized geothermal power technology: dry-steam power generation, which is applied to a dry-steam geothermal resource and accounts for about 27% of all installed geothermal plant capacity; flash power generation, which is applied to wet-steam or water-dominated geothermal resources and accounts for about 61% of all installed geothermal plant capacity; binary cycle power generation, which is applied to intermediate- to low-temperature water-dominated geothermal resources and accounts for about 11% of all installed geothermal plant capacity (Bertani, 2010).

Based on the temperature and properties of the water-dominated geothermal resource, different energy conversion systems can be utilized to maximize the extraction of energy from the geothermal fluid (Franco and Villani, 2009). Net power output, energy efficiency, exergy efficiency, thermal economics and sensitivity have also been theoretically studied (Jalilinasrabady et al., 2012; Rosyidet al., 2010). The flash-binary power system would increase production compared to a single-flash power system. Denizli power plant in Turkey gained 18% in power production by adding a binary cycle system (Dagdas et al., 2005).

However, there are few studies about the match ability between a geothermal resource temperature and a power cycle. Also, most geofluids contain non-condensable gases, and the power output of the plant is affected by the gas mass fraction. There are few studies about a gas-vapour-liquid power plant. This report explores five different types of power system thermodynamic optimizations, including gas-vapour-liquid, and one case of thermoeconomic optimization.

3. THERMODYNAMIC OPTIMIZATION OF A GEOTHERMAL POWER PLANT

Thermodynamics can analyse the power generation from an energy view point; the fundamentals and mathematical model are found in DiPippo (2008). The main components of a flash and binary system are: a separator, a preheater, a vaporizer, a condenser and a turbine (Ahangar, 2012).

3.1 Single-flash system optimization

A single-flash system is the first scenario for Tuo-bei geothermal field; the conditions are shown in Table 3. A throttle valve, a separator, a turbine, a condenser and a cooling tower are the main equipment in the system. The separation pressure P_2 is the main variable used to optimize the turbine power output. Figure 4 shows the diagram of a single-flash system. Figure 5 shows the thermodynamic T-s diagram of the single-flash process.

Optimization focuses on obtaining optimum separation pressures which could maximize power output. Therefore, using the EES program, the separation pressure P_2 was varied in order to find the maximum net power output. The relationship between separation pressure and turbine work, using the second law of efficiency, is shown in Figure 6. The optimum pressure is P_2=0.95 bar; the maximum power, shown on the top of the red curve, is 2301 kW.

Table 4 shows the optimum thermodynamic properties of each process state in a single-flash system. The main results for a single-flash cycle are shown in Table 5. The injection temperature is about 98°C; the first and second laws of efficiency are 7.9% and 34.7%, respectively. The condenser area is about 1212 m^2.

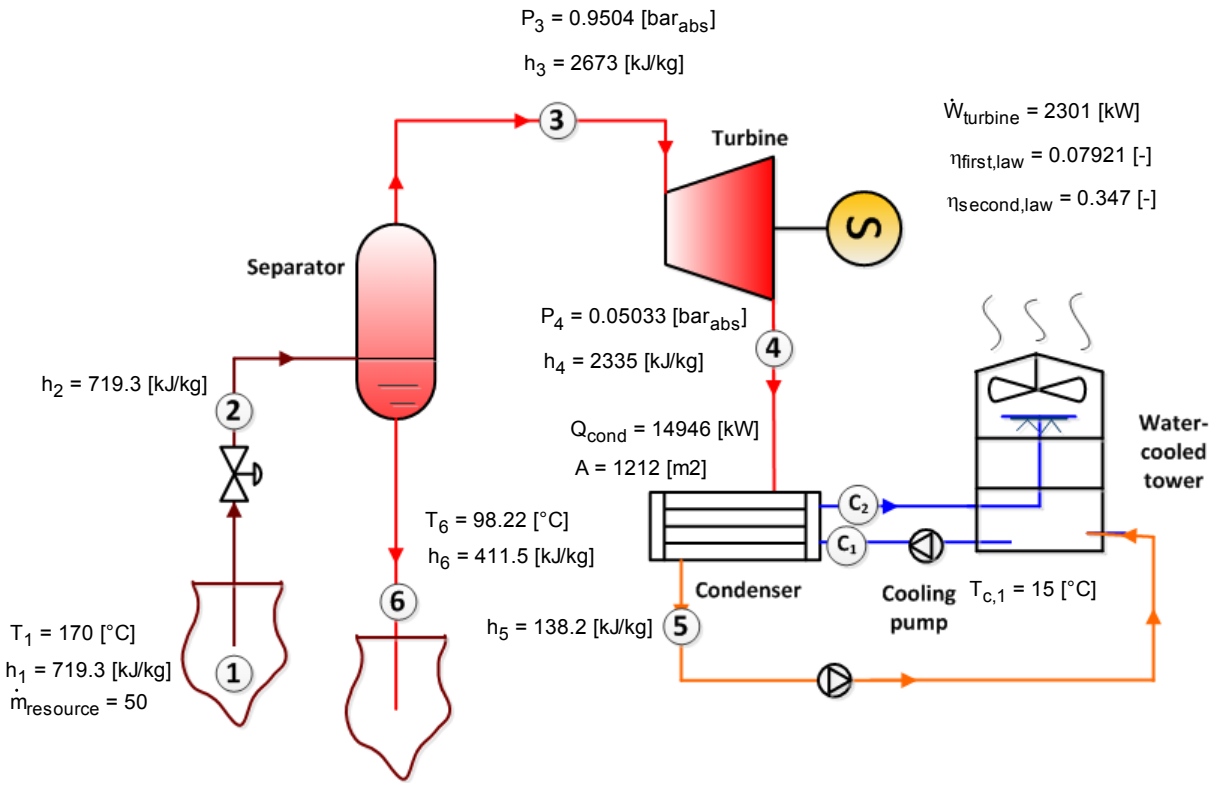

FIGURE 4: Single-flash system diagram

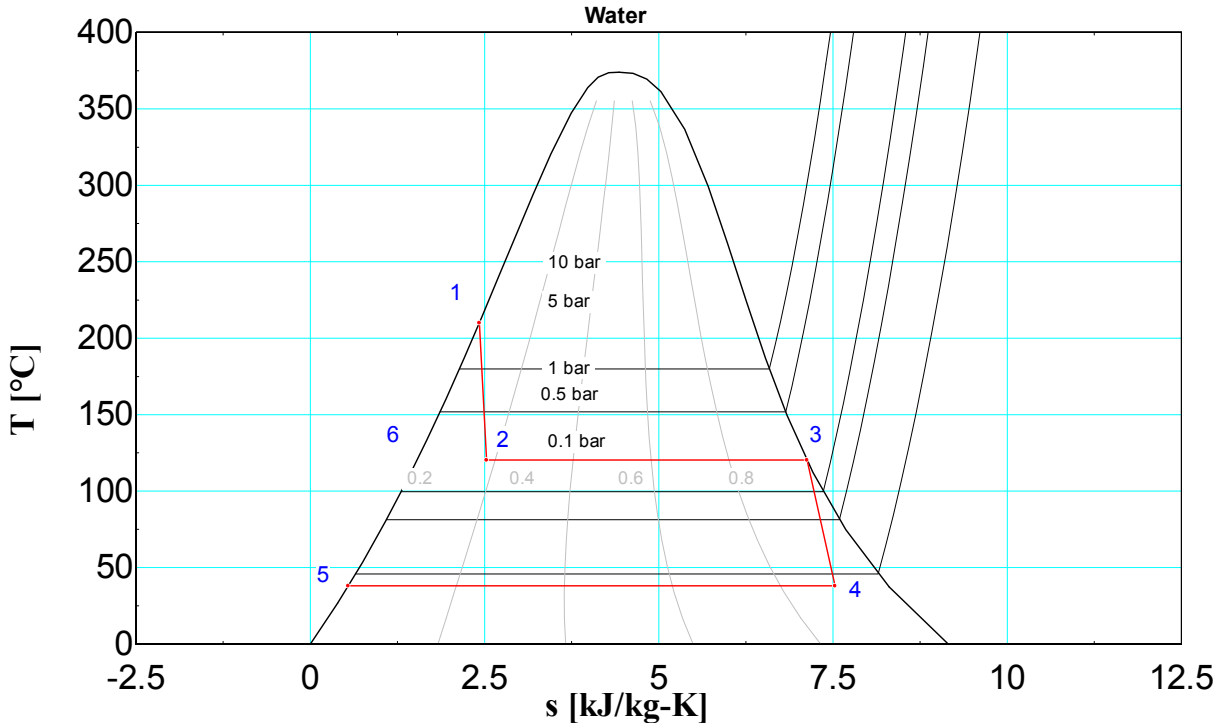

FIGURE 5: Single-flash T-s diagram

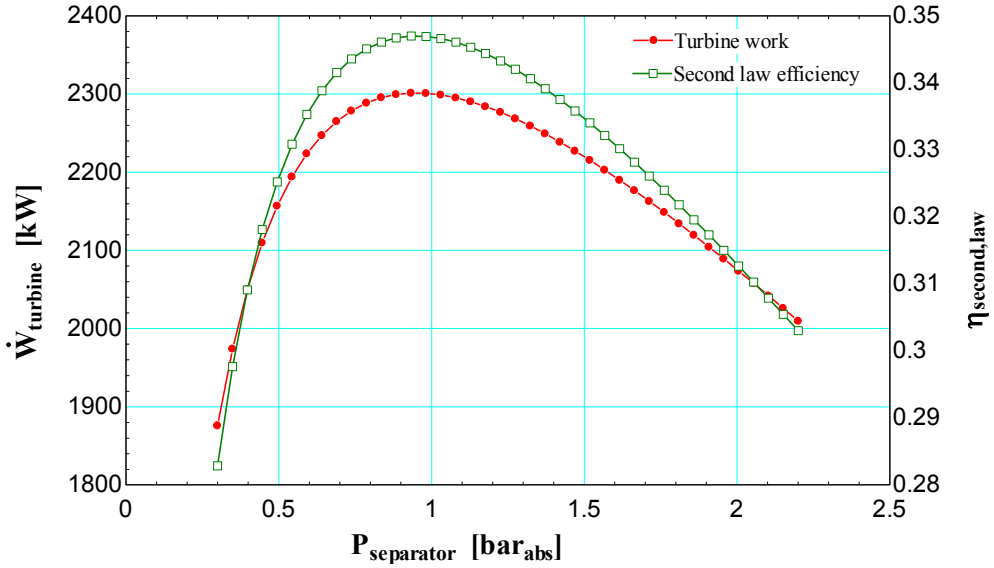

FIGURE 6: Separator pressure and turbine power relationship

TABLE 4: Thermodynamic optimization of single flash

State	Pressure	Temperature	Mass flow	Steam quality	Volume	Enthalpy	Entropy	Heat rate	Specific exergy	Exergy rate
	P (bars)	T (°C)	M (kg/s)	x	v (m^3/kg)	h (kJ/kg)	s (kJ/kg°C)	Q (kW)	e (kJ/kg)	Ex (kW)
1	7.92	170	50.0	0.000	0.001	719	2.04	35965	132.60	6632
2	0.95	98	50.0	0.136	0.243	719	2.12	35965	112.00	5576
3	0.95	98	6.8	1.000	1.777	2673	7.38	18176	550.00	3739
4	0.05	33	6.8	0.907	25.400	2335	7.65	15878	132.00	897
5	0.05	33	6.8	0.000	0.001	138	0.48	938	2.00	15
6	0.95	98	43.2	0.000	0.001	412	1.29	17798	42.00	1837
c1	-	15	357.3		0.001	63	0.22	22510	0.20	71
c2	-	25	357.3		0.001	105	0.37	37481	0.72	259

TABLE 5: Energy summary of single flash

No.	Item	Units	Optimum value
1	Separator pressure	bar	0.95
2	Turbine shaftwork	kW	2301
3	Cooling pump	kW	71.51
4	Turbine net output power	kW	2230
5	Condenser temperature	°C	33
6	Condenser capacity	kW	14946
7	Condenser area	m^2	1212
8	The first law efficiency	%	7.9
9	The second law efficiency	%	34.7

3.2 Binary system optimization

A binary power cycle is the second scenario for Tuo-bei geothermal field; the conditions are shown in Table 3. A vaporizer, apreheater, a working pump, a turbine, a condenser and a cooling tower are the

main components in the system. The vaporizer pressure, preheater pinch and preheater area are the main variables used to optimize the turbine power output. Figure 7 shows the diagram of a single-flash system. Figure 8 shows the thermodynamic T-s diagram of the single-flash process.

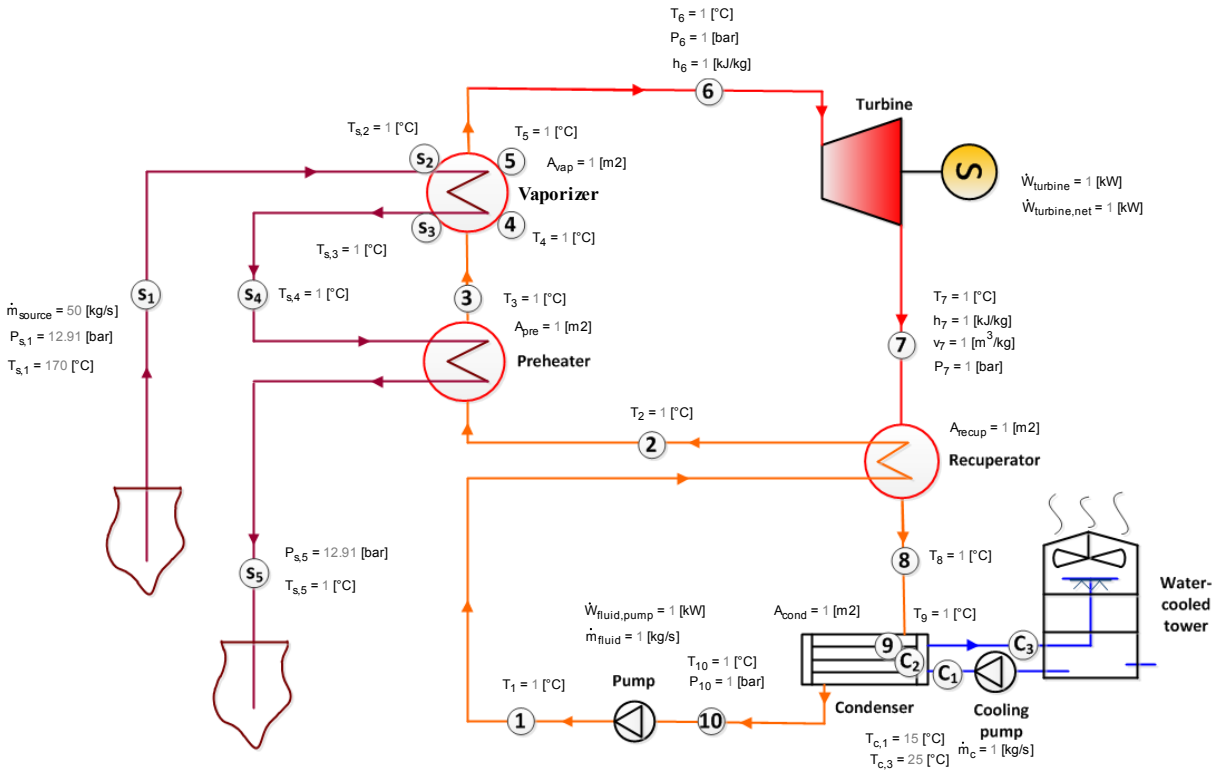

FIGURE 7: Binary system diagram

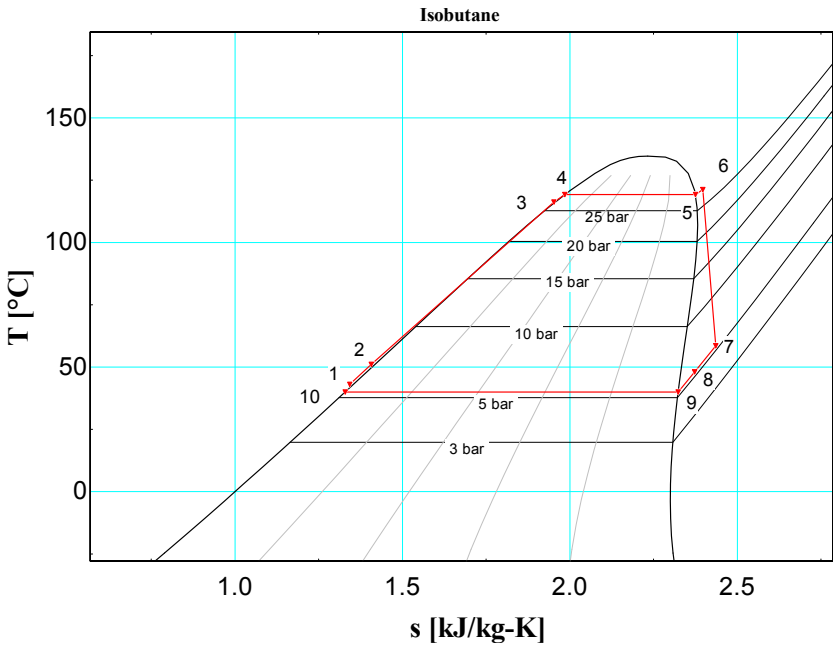

FIGURE 8: Binary T-s diagram

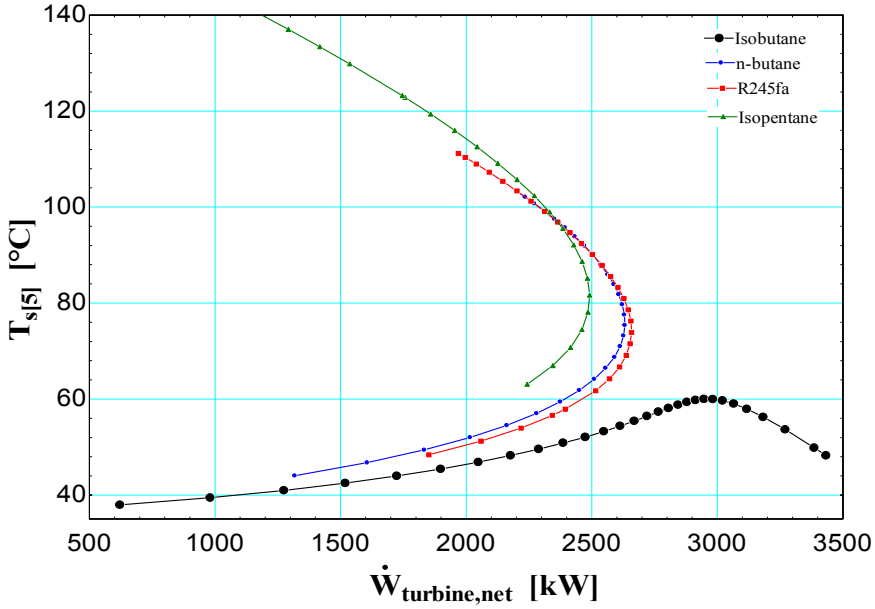

FIGURE 9: The relationship of turbine work and reinjection temperature

Optimization focuses on obtaining the optimum vaporizer pressure. Figure 9 gives the relationship of the turbine work and the injection temperature of four different working fluids. For isobutane, the maximum injection temperature is about 60°C. Therefore, the vaporizer pressure at 28 bar is the optimum vaporizer pressure for a binary cycle. The turbine shaft and net output power are 3506 kW and 3022 kW, respectively.

Figure 10 shows the relationship of efficiency, injection temperature and vaporizer pressure. The value of the first law of efficiency, second law of efficiency and the injection temperature are 12.9%, 45.4% and 59.7°C, respectively.

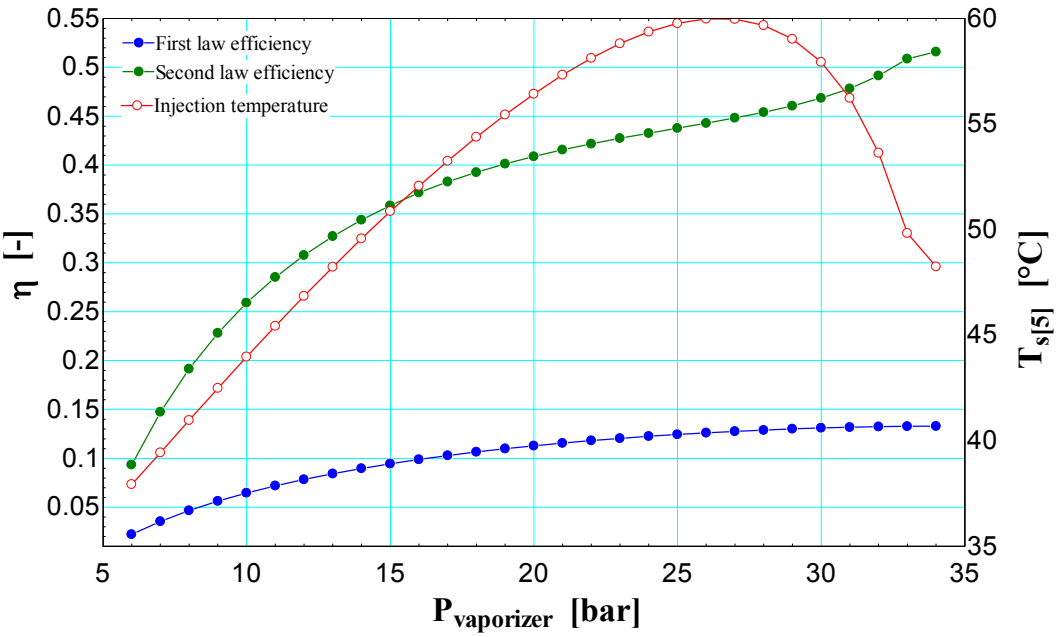

FIGURE 10: The relationship of efficiency, injection temperature and vaporizer pressure

Table 6 shows the optimum thermodynamic properties of each process state in a binary power system. The main results of the binary cycle are shown in Table 7.

TABLE 6: Thermodynamic optimization of a binary system

State	Pressure	Temperature	Mass flow	Steam quality	Volume	Enthalpy	Entropy	Heat rate	Specific exergy	Exergy rate
	P (bars)	T (°C)	m (kg/s)	x	v (m^3/kg)	h (kJ/kg)	s (kJ/kg°C)	Q (kW)	e (kJ/kg)	Ex (kW)
1	28.0	35	62.6	-100	0.002	284	1.274	17799	6.05	368
2	28.0	45	62.6	-100	0.002	311	1.358	19459	8.15	496
3	28.0	117	62.6	-100	0.002	525	1.963	32906	48.83	2971
4	28.0	119	62.6	-100	0.002	534	1.985	33451	51.12	3111
5	28.0	119	62.6	1	0.015	687	2.375	43039	91.78	5585
6	28.0	121	62.6	100	0.016	696	2.397	43578	94.09	5725
7	4.4	53	62.6	100	0.097	638	2.441	39964	23.61	1437
8	4.4	40	62.6	100	0.092	612	2.359	38311	21.00	1278
9	4.4	33	62.6	1	0.089	599	2.317	37497	20.11	1224
10	4.4	33	62.6	-100	0.002	278	1.269	17436	1.60	97
S1	12.9	170	50.0		0.001	720	2.041	35980	133.10	6655
S2	12.9	168	50.0		0.001	709	2.018	35455	129.50	6473
S3	12.9	124	50.0		0.001	523	1.573	26140	71.32	3566
S4	12.9	122	50.0		0.001	512	1.546	25610	68.44	3422
S5	12.9	60	50.0		0.001	251	0.826	12545	14.45	723
C1	-	15	485.0		0.001	63	0.224	30608	0.20	99
C2		25	485.0		0.001	103	0.362	50101	0.67	335
C3	-	25	485.0		0.001	105	0.368	50877	0.72	361

TABLE 7: Energy summary of binary system

No.	Item	Units	Optimum value
1	Vaporizer pressure	bar	28
2	Condenser pressure	bar	4
3	Turbine shaft work	kW	3506
4	Cooling pump	kW	129
5	Working pump	kW	355
6	Turbine net output power	kW	3022
7	Condenser temperature	°C	33
8	Condenser capacity	kW	20284
9	Vaporizer area	m^2	634
10	Preheater area	m^2	2157
11	Recuperator area	m^2	350
12	Condenser area	m^2	1742
13	The first law efficiency	%	13
14	The second law efficiency	%	45

3.3 Double-flash system optimization

The double-flash cycle is the third scenario for Tuo-bei geothermal field; the conditions are shown in Table 3. Two individual turbines are used in the system. The high separation pressure P_2 and low separation pressure P_8 are the main variables used to optimize the turbine power output. Figure 11 shows the diagram of a double-flash system. Figure 12 shows the thermodynamic T-s diagram of the process.

Optimization focuses on obtaining the optimum separation pressures for both separators to maximize power output. Therefore, the two separation pressures, P_2 and $P_{8,}$ were varied, using the EES program, in order to find the maximum net power output. The 3D relationship of high separation pressure, low

separation pressure and turbine work is shown in Figure 13, based on the Scilab programme. The optimum pressures were: P_2=2.08 bar; P_8=0.39 bar. The maximum power is shown, in the top left area, to be 2940 kW.

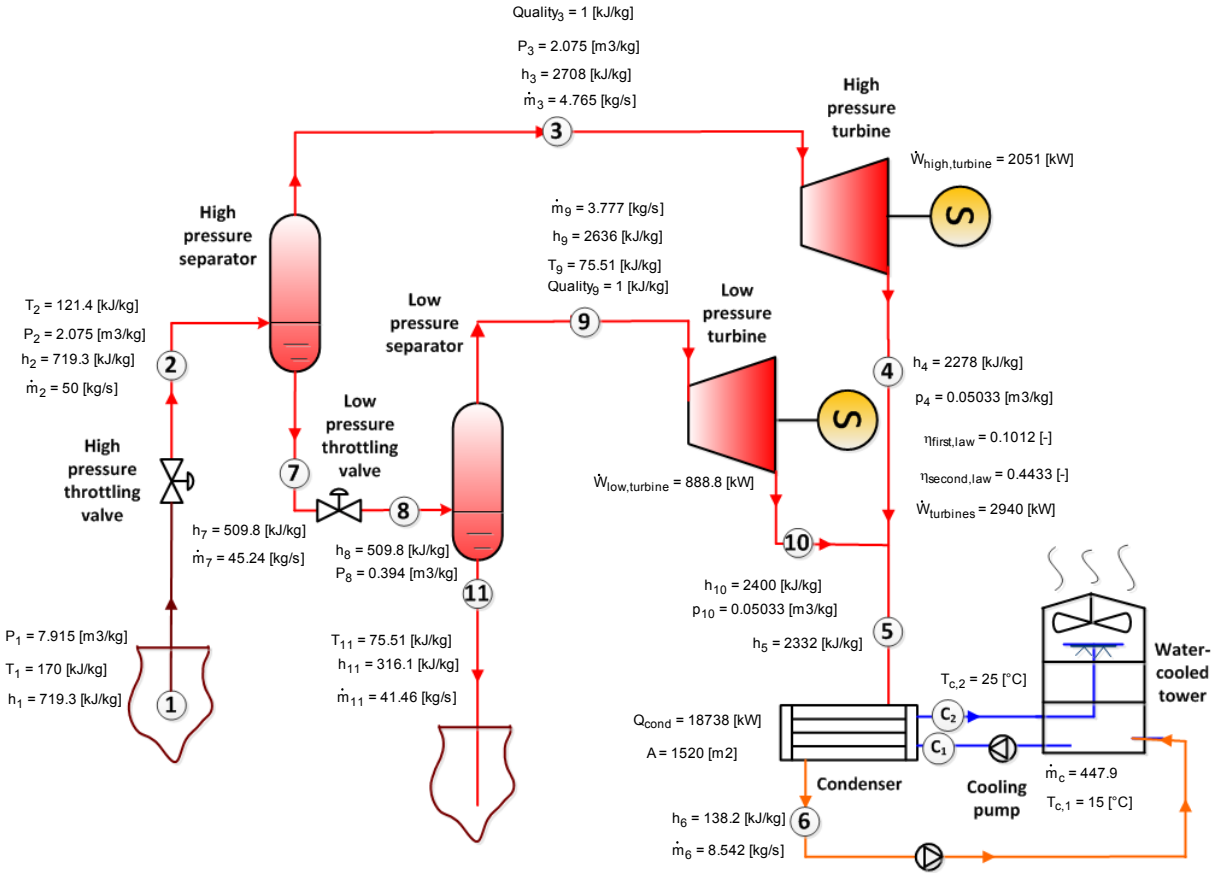

FIGURE 11: Double system diagram

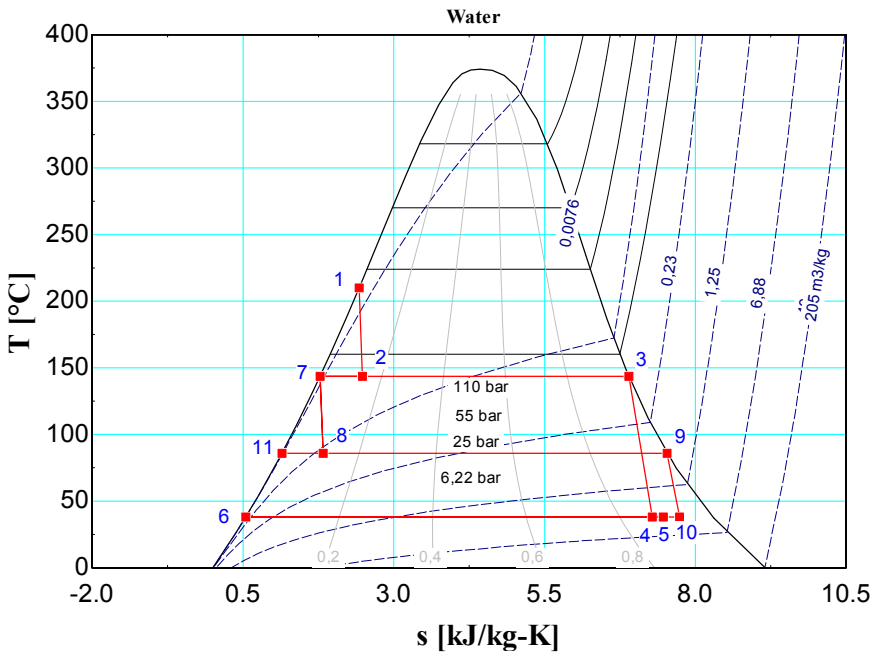

FIGURE 12: Double-flash T-s diagram

Table 8 shows the optimum thermodynamic properties of each process state in a double-flash system. The main results of the double-flash cycle are shown in Table 9. The injection temperature is about 76°C, the first and second laws of efficiency are 10% and 44%, respectively. The condenser area is about 1520 m^2.

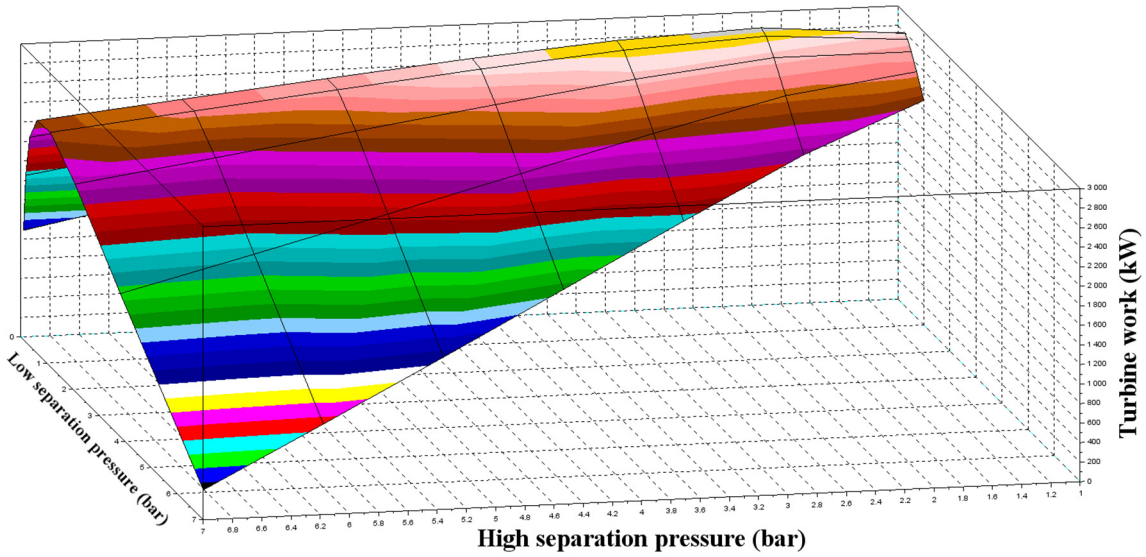

FIGURE 13: Low separator pressure, high separator pressure and turbine power relationship

TABLE 8: Thermodynamic optimization of a double-flash system

State	Pressure	Temperature	Mass flow	Steam quality	Volume	Enthalpy	Entropy	Heat rate	Specific exergy	Exergy rate
	P (bars)	T(°C)	m (kg/s)	x	v (m^3/kg)	h (kJ/kg)	s (kJ/kg°C)	Q (kW)	e (kJ/kg)	Ex (kW)
1	7.92	170	50.0	0.000	0.001	719	2.04	35965	133	6632
2	2.08	121	50.0	0.095	0.083	719	2.07	35965	124	6173
3	2.08	121	4.8	1.000	0.856	2708	7.12	12904	660	3145
4	0.05	33	4.8	0.883	24.740	2278	7.47	10855	128	612
5	0.05	33	8.5	0.906	25.370	2332	7.64	19920	132	1124
6	0.05	33	8.5	0.000	0.001	138	0.48	1181	2	19
7	2.08	121	45.2	0.000	0.001	510	1.54	23063	67	3028
8	0.39	76	45.2	0.083	0.339	510	1.58	23063	57	2582
9	0.39	76	3.8	1.000	4.051	2636	7.67	9956	426	1610
10	0.05	33	3.8	0.934	26.160	2400	7.87	9065	136	512
11	0.39	76	41.5	0.000	0.001	316	1.02	13106	23	972
c1		20	447.9		0.001	63	0.22	28267	0	88
c2		30	447.9		0.001	105	0.37	47030	1	325

TABLE 9: Energy summary of a double-flash system

No.	Item	Units	Optimum value
1	High-pressure separator pressure	bar	2.08
2	Low-pressure separator pressure	bar	0.39
3	High-pressure turbine output power	kW	2051
4	Low pressure turbine output power	kW	889
5	Total turbine shaft work	kW	2940
6	Cooling pump	kW	90
7	Total turbine net output power	kW	2850
8	Condenser temperature	°C	33
9	Condenser capacity	kW	70738
10	Condenser area	m^2	1520
11	The first law efficiency	%	10.12
12	The second law efficiency	%	44.33

3.4 Flash-binary system optimization

A flash-binary system is the fourth scenario for Tuo-bei geothermal field; the conditions are shown in Table 3. Flash and binary turbines are used in this system. The separation pressure P_{10} and vaporizer pressure P_5 are the main variables used to optimize the turbine power output. Figure 14 shows the diagram of a flash-binary system.

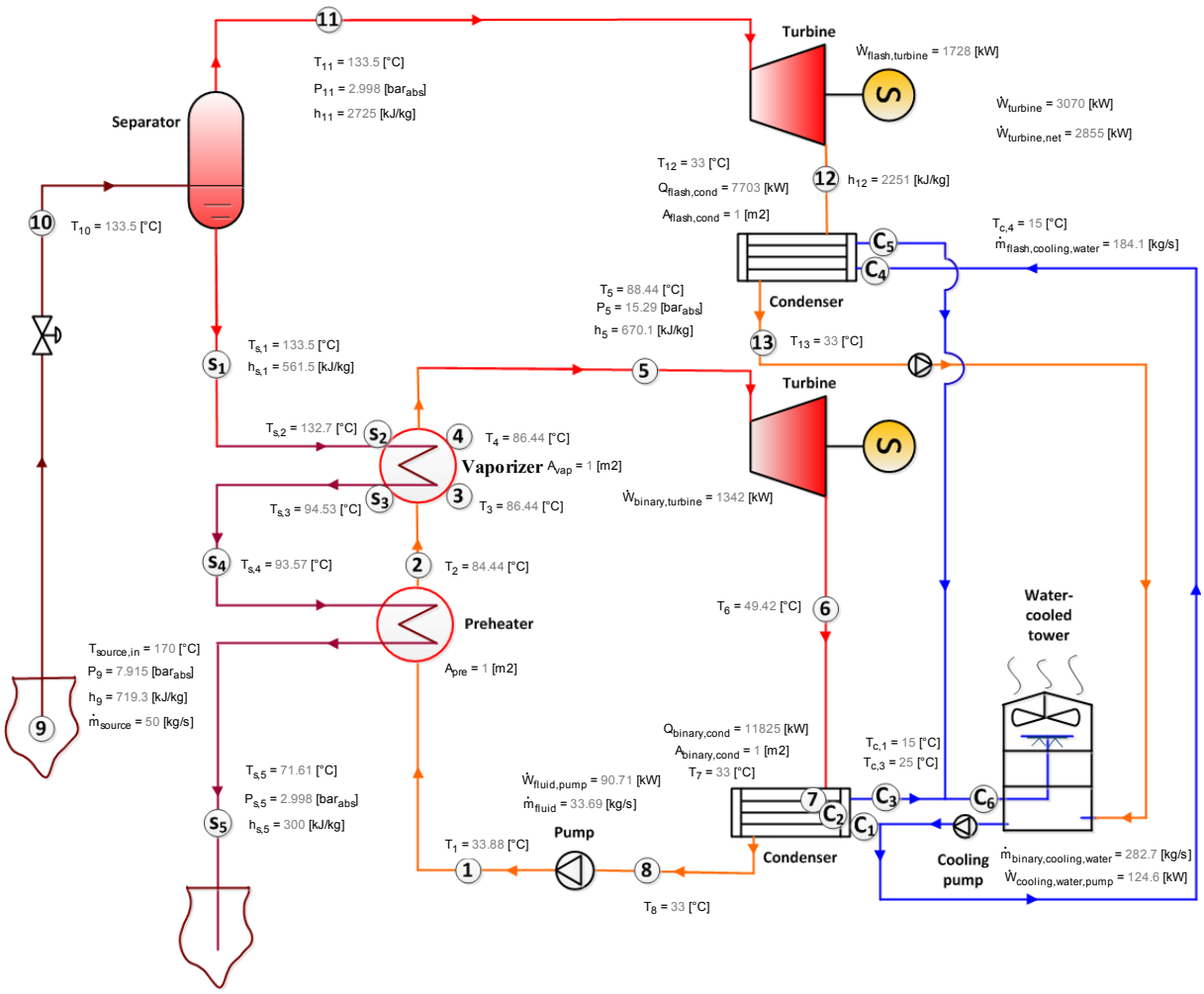

FIGURE 14: Flash-binary system diagram

Optimization focuses on obtaining the optimum separation pressures and vaporizer pressure which could maximize power output. Figure 15 shows the 3D relationship of separation pressure, vaporizer pressure and turbine work, based on the Scilab programme. The optimum pressures are: P_{10}=2.998 bar; P_5=15.29 bar. The maximum power, shown in the top left area, is 3070 kW.

Table 10 shows the optimum thermodynamic properties of each process state in a flash-binary system. The main results of the flash-binary cycle are shown in Table 11. The injection temperature is about 72°C. The area of the flash condenser, the binary condenser, the preheater and the vaporizer are about 625 m^2, 971 m^2, 382 m^2 and 327 m^2, respectively.

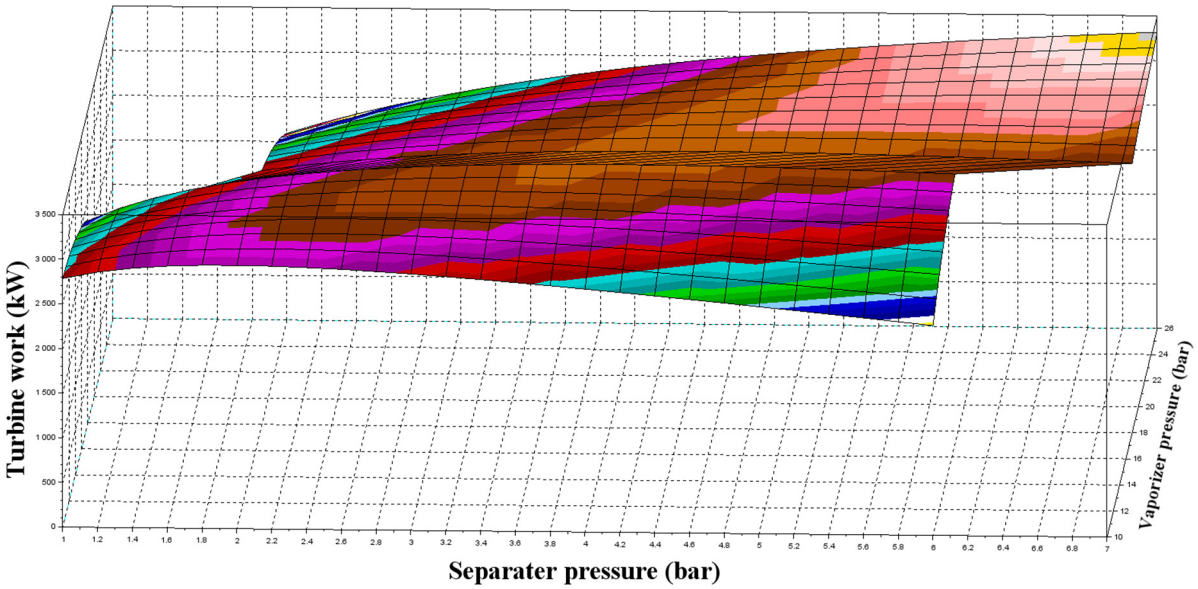

FIGURE 15: Separator pressure, vaporizer pressure and turbine power relationship

TABLE 10: Thermodynamic optimization of a flash-binary system

State	Pressure	Temperature	Mass flow	Steam quality	Volume	Enthalpy	Entropy	Heat rate	Specific exergy	Exergy rate
	P (bars)	T (°C)	m (kg/s)	x	v (m^3/kg)	h (kJ/kg)	s (kJ/kg.°C)	Q (kW)	e (kJ/kg)	Ex (kW)
1	15.29	34	33.7	-100	0.002	282	1.27	9501	3.72	125
2	15.29	84	33.7	-100	0.002	419	1.69	14106	21.94	739
3	15.29	86	33.7	0.00	0.002	425	1.70	14312	23.13	779
4	15.29	86	33.7	1.00	0.024	665	2.37	22404	70.87	2388
5	15.29	88	33.7	100	0.025	670	2.39	22576	71.91	2423
6	4.40	49	33.7	100	0.095	630	2.42	21235	23.10	778
7	4.40	33	33.7	1.00	0.088	599	2.32	20187	20.51	691
8	4.40	33	33.7	0.00	0.002	279	1.27	9410	1.66	56
9	7.92	170	50.0	100	0.001	719	2.04	35965	132.60	6632
10	3.00	134	50.0	0.07	0.045	719	2.06	35965	127.50	6377
11	3.00	134	3.6	100	0.606	2725	6.99	9935	712.40	2597
12	0.05	33	3.6	100	24.430	2251	7.38	8207	126.90	463
13	0.05	33	3.6	100	0.001	138	0.48	504	2.27	8
S1	3.00	134	46.4		0.001	562	1.67	26026	81.53	3779
S2	3.00	133	46.4	-100	0.001	558	1.66	25868	80.53	3733
S3	3.00	95	46.4	-100	0.001	396	1.25	18364	39.31	1822
S4	3.00	94	46.4	-100	0.001	392	1.23	18174	38.44	1782
S5	3.00	72	46.4	-100	0.001	300	0.97	13905	20.94	971
C1	2	15	282.7		0.001	63	0.22	17841	0.20	93
C2	-	24	282.7			101	0.36	28609	0.60	171
C3	-	25	282.7			105	0.37	29655	0.72	205
C4	2	15	184.1		0.001	63	0.22	11619	0.20	37
C5	-	25	184.1		0.001	105	0.37	19312	0.72	133
C6	-	25	466.8		0.001	105	0.37	48967	0.72	338

TABLE 11: Energy summary of a flash-binary system

No.	Item	Units	Optimum value
1	Separator pressure	bar	2.998
2	Vaporizer pressure	bar	15.29
3	Flash turbine shaft work	kW	1728
4	Binary turbine shaft work	kW	1342
5	Total turbine shaft work	kW	3070
6	Working fluid pump	kW	91
7	Cooling pump	kW	125
8	Total turbine net output power	kW	2855
9	Injection temperature	°C	72
10	Flash condenser capacity	kW	7703
11	Flash condenser area	m^2	624.7
12	Binary condenser capacity	kW	11852
13	Binary condenser area	m^2	971
14	Vaporizer area	m^2	382.3
15	Preheater area	m^2	326.6

3.5 Gas-vapour-liquid binary system optimization

The gas-vapour-liquid binary system is just suitable for Yu-Lingong geothermal field, which includes 8% non-condensable gas; the conditions are shown in Table 3. Two separators and one gas-vapour vaporizer are used in the system. The first separation pressure P_{g1} and vaporizer pressure P_{12} are the main variables used to optimize the turbine power output. Figure 16 shows the diagram of a gas-vapour-liquid binary system.

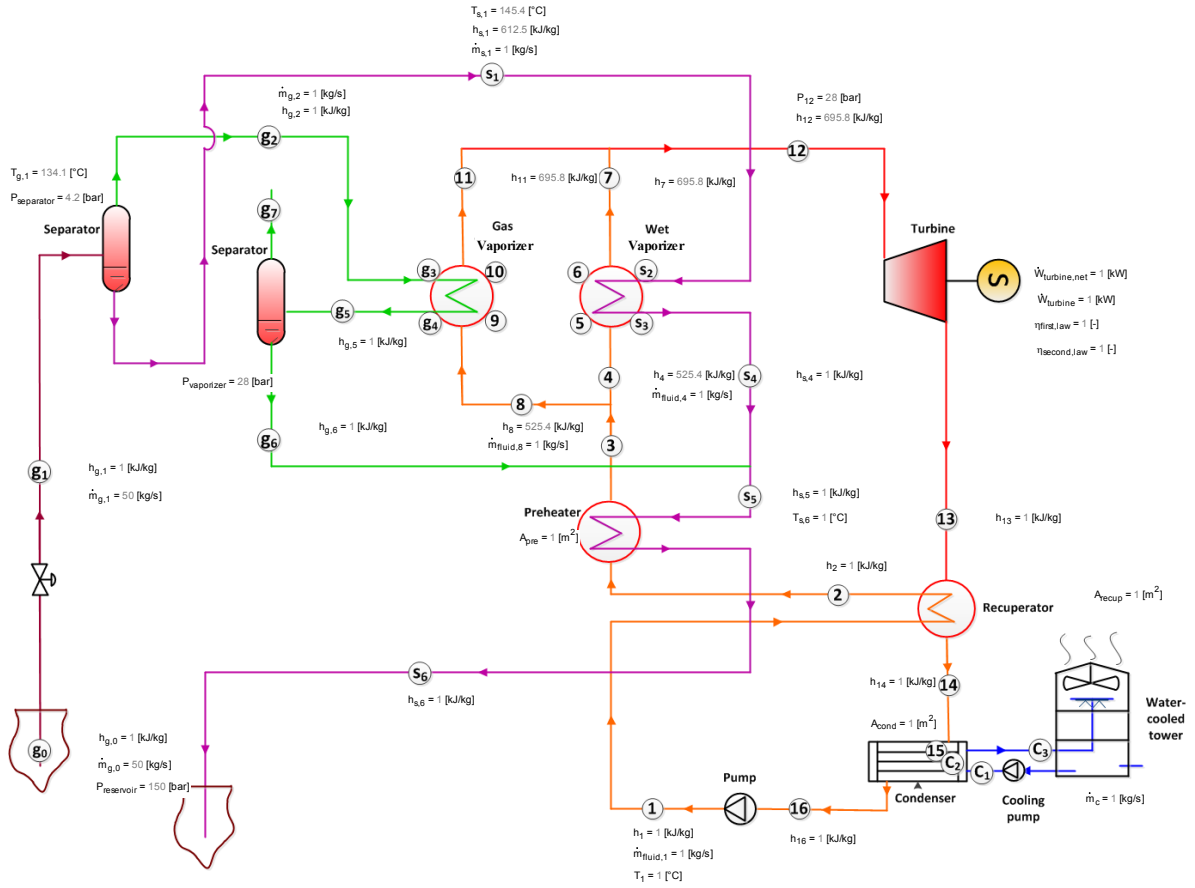

FIGURE 16: Gas-vapour-liquid binary system diagram

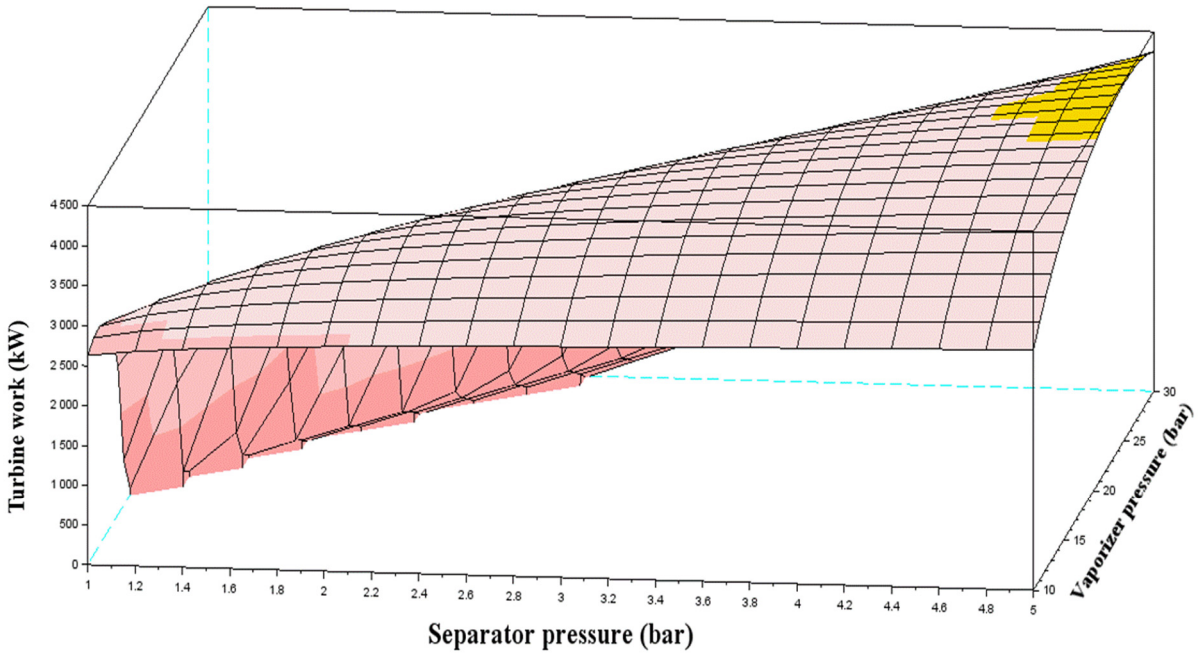

FIGURE 17: Separator pressure, vaporizer pressure and turbine power relationship of a gas-vapour-liquid binary system

Figure 17 gives the relationship of the separator pressure, vaporizer pressure and turbine power. The greater the separator and vaporizer pressure, the bigger the turbine work. However, the optimum thermodynamic parameters are affected by other factors. The constricting conditions are as follows: the maximum turbine work; the preheater pinch; the temperature pinch between T_{s6} and T_2 is more than 15°C; and the injection temperature T_{s6} is between 50 and 60°C. Figure 18 gives the relationship of the vaporizer pressure and the injection temperature T_{s6} at a separator pressure of 4.2 bar. Therefore, the optimum separator and vaporizer pressure are 4.2 bar and 28 bar, respectively.

Table 12 shows the optimum thermodynamic properties of each process state in a gas-vapour-liquid binary system. The main results of the gas-vapour-liquid binary cycle are shown in Table 13. The injection temperature is about 51.85°C. The total turbine shaft work is 3773 kW, the areas of the gas-vapour vaporizer, wet vaporizer, preheater, recuperator and condenser are 662 m^2, 341 m^2, 1988 m^2, 360 m^2 and 5160 m^2, respectively.

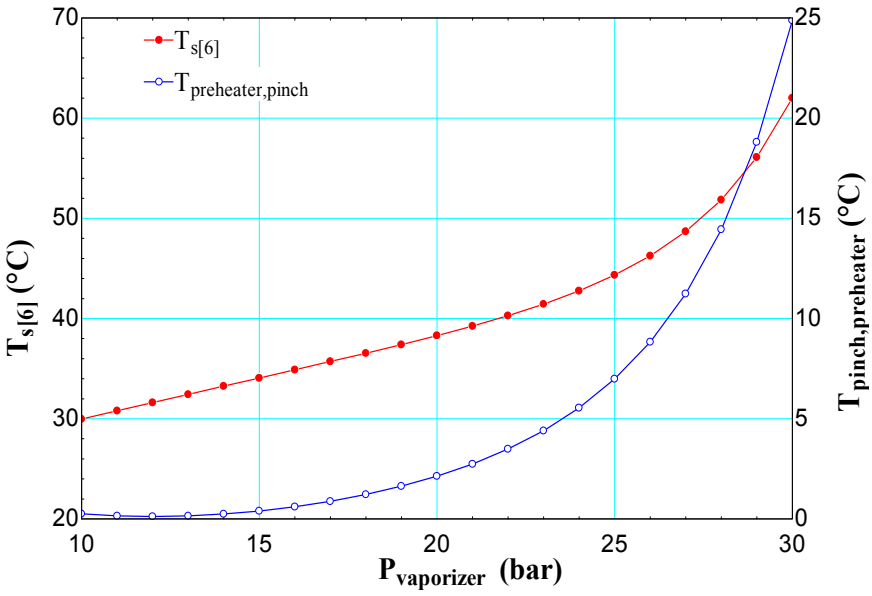

FIGURE 18: Vaporizer pressure, T_{s6} and preheater temperature pinch relationship

TABLE 12: Thermodynamic optimization of a gas-vapour-liquid binary system

State	Pressure	Temperature	Mass flow	Volume	Enthalpy	Entropy	Heat rate	Specific exergy	Exergy rate
	P (bars)	T (°C)	m (kg/s)	v (m^3/kg)	h (kJ/kg)	s (kJ/kg.°C)	Q (kW)	e (kJ/kg)	Ex (kW)
1	28.0	25	56.6	0.002	261	1.20	14744	4.9	277
2	28.0	37	56.6	0.002	291	1.30	16493	6.5	370
3	28.0	117	56.6	0.003	525	1.96	29738	48.8	2764
4	28.0	117	23.4	0.003	525	1.96	12268	48.8	1140
5	28.0	119	23.4	0.003	534	1.99	12471	51.1	1194
6	28.0	119	23.4	0.011	687	2.38	16046	91.8	2144
7	28.0	121	23.4	0.011	696	2.40	16247	94.1	2197
8	28.0	117	33.3	0.003	525	1.96	17470	48.8	1623
9	28.0	119	33.3	0.003	534	1.99	17759	51.1	1699
10	28.0	119	33.3	0.011	687	2.38	22849	91.8	3051
11	28.0	121	33.3	0.011	696	2.40	23135	94.1	3128
12	28.0	121	56.6	0.011	696	2.40	39382	94.1	5325
13	3.3	47	56.6	0.129	629	2.45	35607	12.2	691
14	3.3	30	56.6	0.120	598	2.35	33864	9.9	560
15	3.3	23	56.6	0.116	586	2.31	33162	9.4	533
16	3.3	23	56.6	0.002	255	1.19	14410	0.4	22
S1	4.2	145.4	41.7		613	1.80	25523	97.0	4043
S2	4.2	144.3	41.7		608	1.78	25323	95.5	3980
S3	4.2	124.2	41.7		522	1.57	21748	70.4	2934
S4	4.2	123.1	41.7		517	1.56	21543	69.1	2878
S5	4.2	123.1	44.2		517	1.56	22861	69.1	3054
S6	4.2	51.85	44.2		217	0.73	9611	9.5	421
g0	150.0	180	50.0		714	1.93	35690	160.2	8011
g1	4.2	134.1	50.0		714	2.02	35690	132.6	6629
g2	4.2	134.2	8.3		1463	3.75	12182	383.8	3195
g3	4.2	133.8	8.3		1429	3.67	11899	373.9	3113
g4	4.2	124.2	8.3		818	2.15	6808	199.8	1664
g5	4.2	123.2	8.3		783	2.06	6520	190.3	1585
g6	4.2	123.2	2.5		518	1.56	1310	69.0	175
g7	4.2	123.2	5.8		899	2.28	5210	243.4	1410
C1	2.0	15	465.0	0.001	63	0.22	29346	0.2	92
C2	-	24.64	465.0	0.001	103	0.36	48081	0.7	314
C3	-	25	465.0	0.001	105	0.37	48779	0.7	337

TABLE 13: Energy summary of a gas-vapour-liquid binary system

No.	Item	Units	Optimum value
1	Vaporizer pressure	bar	28
2	Separator pressure	bar	4.2
3	Turbine shaft work	kW	3773
4	Cooling pump	kW	124.1
5	Working pump	kW	337.4
6	Turbine net output power	kW	3311
7	Condenser temperature	°C	24.6
8	Condenser capacity	kW	19453
9	Gas-vapour-liquid vaporizer area	m^2	661.7
10	Wet vaporizer area	m^2	341.8
11	Preheater area	m^2	1988
12	Recuperator area	m^2	360
13	Condenser area	m^2	5160
14	The first law efficiency	%	13.4
15	The second law efficiency	%	50

3.6 Comparison of different power systems

The calculations and optimization of four power plant scenarios were carried out for Tuo-bei geothermal field, as well as a gas-vapour-liquid binary system for Yu-lingong geothermal field. The main results for the Tuo-bei power systems are summarized in Table 14. Later in this report, the five scenarios for Tuo-bei geothermal field will be compared.

TABLE 14: Power system design comparison for Tuo-bei field

Item	Unit	Single flash	Binary cycle	Double flash	Flash-binary combined system	Gas-vapour-liquid binary system
W_{net}	kW	2230	3022	2850	2855	3311
$T_{injection}$	°C	98	60	76	72	52
A_{total}	m^2	1212	4583	1520	2305	8511
η_{first}	%	7.9	13	10	-	13.4
η_{second}	%	34.7	45	44	-	50

A binary system offers the maximum net power output and second law of efficiency. The total area of the binary system is the largest of the four scenarios, but an additional separator would be used in the other three scenarios. Therefore, a binary power system will be designed for Tuo-bei geothermal field. In Chapter 4, the economics of a binary system will be discussed.

4. THERMOECONOMIC OPTIMIZATION OF A GEOTHERMAL BINARY POWER PLANT

4.1 Methodology and process

The economic evaluation and analysis of a binary power plant were implemented by using the engineering economic methodology. There are three methods for economic evaluation (Bejan and Moran, 1996; Sun, 2008).

a) The first is based on the average rate of return and payback period method. The payback period is defined as the length of time required for cash inflows received from the project to recover the original cash outlays required by the initial investment.

b) The second is the Net Present Value (NPV) method. When the net present value method is used for project selection, the following rules apply: accept any project for which the present value is positive; reject any project with negative present value; the project with the highest present value is given the highest preference among various alternatives; if two projects are mutually exclusive, accept the one having the greater present value.

c) The third is the internal rate of return method. The net present value method uses the interest rate, usually based on the company's cost of money. The internal rate of return method seeks to avoid the arbitrary choice of an interest rate; instead, it calculates an interest rate, initially unknown, that is internal to the project.

The economic conditions of the Tuo-bei geothermal binary power system are shown in Table 15. The exchange rate of Chinese Yuan for U.S. dollar is 6.5 Yuan per dollar in this report.

TABLE 15: Economic conditions of the Tuo-bei binary power plant

No.	Item	Unit	Value
1	Economic life span	year	25
2	Minimum attractive rate of return	%	10
3	Operation time for one year	h	8000
4	Income tax rate	%	17
5	Price of electricity for user	$/kWh	0.09
6	Effective rate of return	%	10

4.2 Cost estimation and cash flow of power plant

The cost estimation of the binary system is shown in Table 16 (Bejan and Moran, 1996). The cooling tower cost is obtained from the Cooling Tower Depots. Total initial investment cost is the sum of the total capital cost and fuel cost: 9,767,000 US$. Figure 19 shows the cash flow of the binary power system. The average annual profit is 1,308,000 $/year, the average rate of return (ARR) is 13.4%, and the payback period is about 6 years. The main results are shown in Table 17.

TABLE 16: Binary power system cost

Item		Capacity	Unit	US$/unit	Cost ($)
PEC	Vaporizer	634	m^2	300	52,310
	Preheater	2157	m^2	300	139,360
	Recuperator	350	m^2	300	32,555
	Condenser	1742	m^2	280	109,654
	Organic fluid turbine	3506	kW	1000	302,977
	Working fluid Pump	355	kW	500	54,892
	Cooling water pump	129	kW	400	19,571
	Cooling tower				210,000
Purchased equipment costs (PEC):					**921,319**
Purchased equipment installation		33%	%PEC		304,035
Piping		35%	%PEC		322,462
Instrumentation and controls		12%	%PEC		110,558
Electrical equipment and materials		13%	%PEC		119,772
Land, Civil, structural		21%	%PEC		193,477
Direct cost					**1,972,000**
Indirect cost (engineering, construction)		15%	%DC		**295,744**
Total capital cost					**2,267,000**
Fuel cost		50	kg/s	150,000	7,500,000
O & M cost		3%	%TCC (per year)		68,021

TABLE 17: Results of cash flow analysis

No.	Item	Unit	Value
1	Average annual profit	$/year	1,308,000
2	Average rate of return	%	13.39
3	Payback period	year	5.73

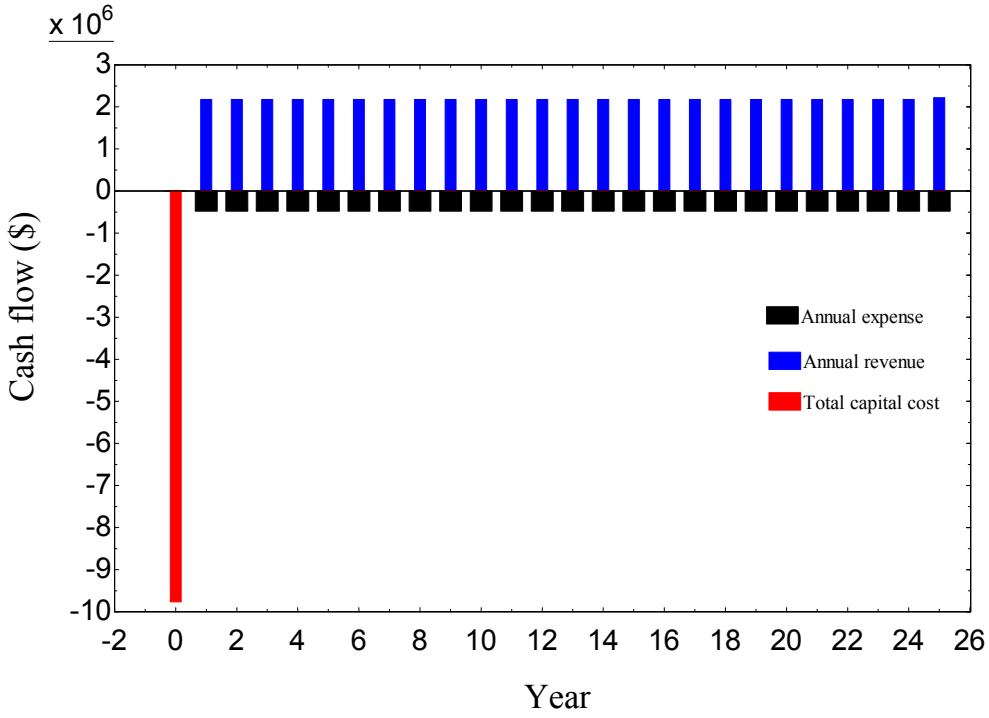

FIGURE 19: Cash flow of a binary power system

4.3 Exergy cost and thermoeconomic optimization

Thermoeconomics deal with the value of the energy within a plant. The analysis is based on exergy flows, and breaks the plant up into individual components, where each component can be analysed separately. The cost flow of products must be equal to the sum of all incoming cost flows for a power system and its components. In thermodynamics, the heat flow is usually considered as input, and work (power) as output. That is the reason for entering the heat cost flow as input and the work (power) cost flow as output. This balance is written as (Valdimarsson, 2011):

$$\sum_{e} \boldsymbol{C_{e,k}} + \boldsymbol{C_{w,k}} = \boldsymbol{C_{q,k}} + \sum_{i} \boldsymbol{C_{i,k}} + \boldsymbol{Z_k} \tag{1}$$

where $\boldsymbol{C}$ = Cost rate ($/s);
$\boldsymbol{Z}$ = Investment cost rate ($/s);
$\boldsymbol{e}$ = Product or output (index);
$\boldsymbol{i}$ = Feed or input (index);
$\boldsymbol{k}$ = Number of components (index);
$\boldsymbol{q}$ = Heat (index);
$\boldsymbol{w}$ =Work or power (index).

4.3.1 Exergy costs

An exergy analysis model was built based on the binary system. Table 18 shows the investment cost rate and destructive exergy cost rate of the main components in the binary system. Each point of exergy cost and unit exergy cost is calculated from the exergy and exergy cost balance. Table 19 shows the results of each point in the binary system.

TABLE 18: Exergy cost rate of the main components in the binary system

Component	Capital cost rate (US$/s)	O&M cost rate (US$/s)	Destruction cost rate (US$/s)
Vaporizer	0.0002164	0.00002403	0.005389
Preheater	0.0005766	0.00006402	0.002515
Recuperator	0.0001347	0.00001495	0.0003483
Working pump	0.0002271	0.00002522	0.0009479
Condenser	0.0004537	0.00005037	0.0104
Turbine	0.001254	0.0001392	0.008794

TABLE 19: Cost rate and unit exergy cost of the binary system

State	Exergy rate	Cost rate	Unit exergy cost	Unit exergy cost
	Ex (kW)	C (US$/s)	c (US$/kWh)	c (US$/kJ)
1	368	0.02275	0.2223	0.00006176
2	496	0.0243	0.1764	0.000049
3	2971	0.03658	0.04432	0.00001231
4	3111	0.0372	0.04305	0.00001196
5	5585	0.04997	0.03221	0.000008947
6	5725	0.05076	0.03192	0.000008865
7	1437	0.01274	0.03192	0.000008865
8	1278	0.01133	0.03192	0.000008865
9	1224	0.01133	0.03332	0.000009257
10	97	0.01183	0.4378	0.0001216
S1	6655	0.02869	0.01552	0.000004311
S2	6473	0.0279	0.01552	0.000004311
S3	3566	0.01537	0.01552	0.000004311
S4	3422	0.01475	0.01552	0.000004311
S5	723	0.003115	0.01552	0.000004311
C1	99	0	0	0
C2	335	0	0	0
C3	361	0	0	0
Power prod.	3506	0.03942	0.04047	0.00001124

4.3.2 Thermoeconomic evaluation

A detailed thermoeconomic evaluation of the binary system should be based on the following variables: exergetic efficiency; exergetic destruction and loss ratio; relative cost difference; and the exergoeconomic factor (Dorj, 2005). The results of the designed power plant are calculated based on a binary system. The main results are shown in Table 20.

TABLE 20: Thermoeconomic evaluation of main components in the binary system

Component	Sum cost rate of destruction and capital investment	Exergetic efficiency	Relative cost difference	Exergetic destruction	Exergetic loss ratio
	(US$/s)	(%)	-	(%)	(%)
Condenser	0.1133	21.6	12.71	13.91	3.832
Turbine	0.01019	81.76	0.1901	11.76	-
Working pump	0.00546	76.27	0.2346	1.267	-
Vaporizer	0.004491	85.17	0.05761	7.2	-
Preheater	0.003395	91.71	0.3685	3.362	10.86
Recuperator	0.001668	80.47	0.02698	0.47	-

4.3.3 Thermoeconomic optimization

The main purpose of thermoeconomic optimization is to achieve a balance between the expenditure on capital costs, and the exergy costs which will lead to a minimum cost of the plant product. The different components in the power system can be categorised as (Dorj, 2005):

1) "Ready-made" components selected from a manufacturer's catalogue, such as pumps, turbines, etc.
2) Components specially designed, or "tailor-made" for the plant, e.g. heat exchangers, etc.

The first type of component is decided by a manufacturer. The second type of component is suitable for thermoeconomic optimization. The advantage of using the exergy method of thermoeconomic optimization is that the various elements of the plant can be optimized on their own; the effect of the given element on the whole plant can be taken into account by local unit costs of exergy fluxes or those of exergy losses.

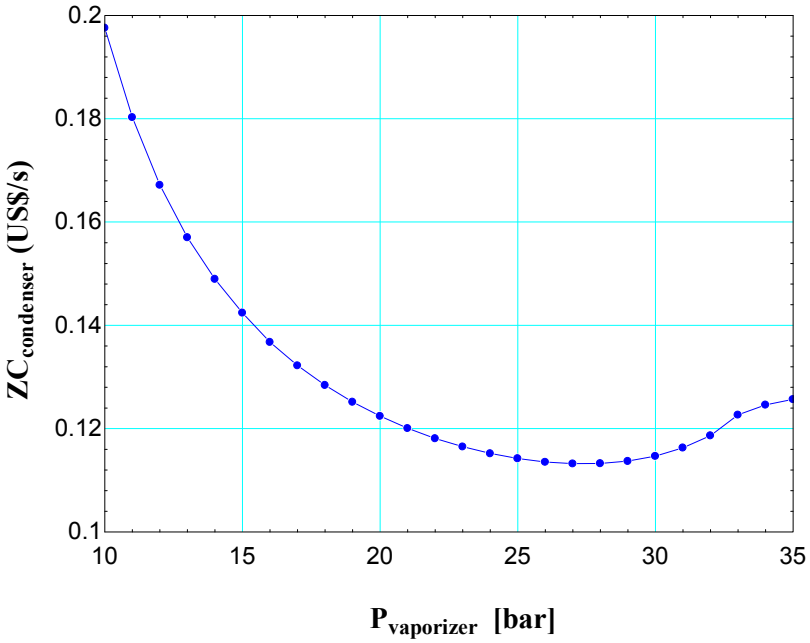

FIGURE 20: Vaporizer pressure and destruction and capital investment total cost rate of condenser

Figure 20 shows the relationship between the vaporizer pressure and the total cost rate of destruction and capital investment for the condenser. The vaporizer pressure affects the sum of the cost rate of destruction and capital investment for the condenser; the minimum value of the cost rate for the condenser is 0.1132, and the vaporizer pressure is 27.4 bar. So the optimum vaporizer pressure is 27.4 bar for thermoeconomic optimi-zation.

4.4 Sensitivity analysis

The geothermal water reservoir temperature and flow rate can affect the power production cost and specific net power output (Dorj, 2005; Estévez, 2012). When the mass flow rate is 50 kg/s, Figure 21 shows the reservoir temperature sensitivity to the power production cost and specific net power output for the binary system. For Tuo-bei geothermal field, the power production cost is about 0.04 US$/kWh.

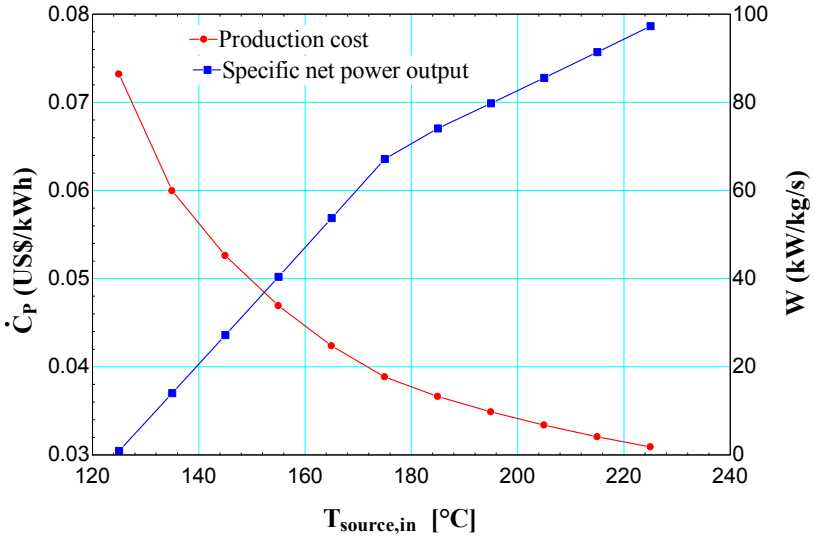

FIGURE 21: Source temperature sensitivity to power production cost and specific net power output

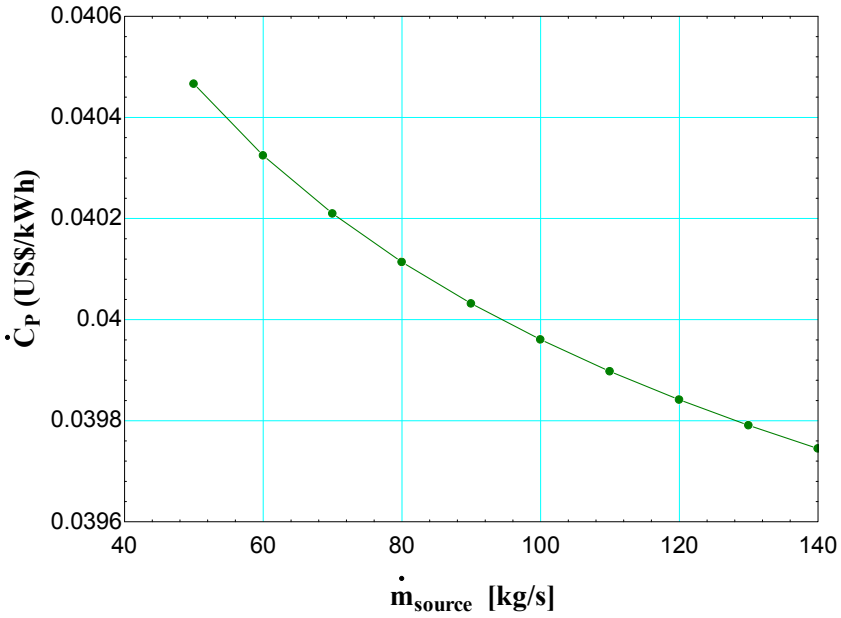

The specific net power output (blue line) increases with reservoir temperature. For Tuo-bei geothermal field, the specific net power output is about 59.76 kW/kg/s. Figure 22 shows the mass flow rate, which affects the power production cost, at a geothermal temperature of 170°C. The power production cost decreases by increasing the mass flow rate.

FIGURE 22: Mass flow rate sensitivity to power production cost

4.5 Economic feasibility based on PV value method

Based on the cash flow of the binary power system, the internal rate of return can be carried out (Sun, 2008). Figure 23 shows the curve of NPV as a function of the internal rate of return in the expected life span. When the NPV equals zero, the maximum internal rate of return is 17.02%. If the internal rate of return equals the average rate of return (13.39%), the NPV is 2,345,000$, which is more than zero. Therefore, economically, a binary power system is feasible for Tuo-bei geothermal field.

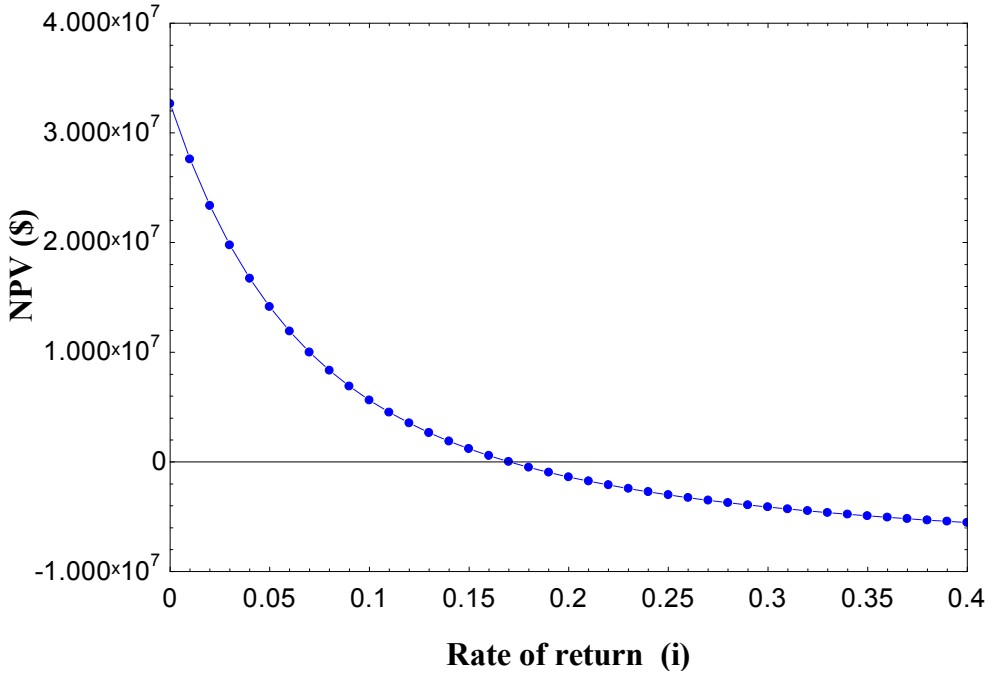

FIGURE 23: Relationship between NPV and internal rate of return

5. CONCLUSIONS

A new geothermal power plant is scheduled to be built in Sichuan Province in China. Five types of geothermal power systems were designed for the Sichuan geothermal area. Based on the thermodynamic and thermoeconomic analysis, the conclusions are as follows:

1) A new geothermal power plant was selected for the Sichuan geothermal area based on the demands of the energy company, and in accordance with government policies. The temperatures of Tuo-bei and Yu-lingong geothermal fields are more than 150°C. The fields are located far from cities. Because of lack of electricity, a geothermal power plant could improve the living standard of the local people.

2) Single-flash, binary cycle, double-flash and single-flash-binary combined power systems were designed for Tuo-bei field. A gas-vapour-liquid binary system was designed for Yu-linggong field. Based on a thermodynamic optimization analysis for these power systems, a binary cycle with a recuperator was selected for Tuo-bei field; the capacity of the power plant is 3506 kW. A gas-vapour-liquid binary system was designed for Yu-lingong field; the capacity of this power plant is 3773 kW.

3) The economic feasibility of a binary cycle with a recuperator was analysed, based on the payback period and NPV methods. The total capital investment is about 20,728,000 US$, with a payback period of less than six years. When the internal rate of return is more than 17%, the net present value is less than zero.

4) Vaporizer pressure is the key variable parameter for a binary system, Thermoeconomic optimization of the main components in a binary power system shows that the condenser destruction and exergy loss is more than that of other components. The optimum pressure is 27.4 bar for Tuo-bei geothermal field.

5) The reservoir temperature and mass flow rate are sensitive for the power production cost. The higher the temperature and the larger the flow rate, the lower the power production cost. For the binary power system in Tuo-bei geothermal field, the power production cost is 0.04 US$/kWh.

ACKNOWLEDGEMENTS

I would like to thank UNU-GTP for the support for this training. Thanks to Mr. Lúdvík S. Georgsson and Mr. Ingimar G. Haraldsson for giving me the precious study opportunity.

I would like to express the deepest and sincerest gratitude to my supervisor, Dr. Páll Valdimarsson. Thanks are extended for his selfless help during my project study.

Thanks to UNU-GTP staff for giving me a family feeling. Thanks for the friendship of our group.

Finally, I would like to express my deepest appreciation to my family. Thanks to my wife for her support and to my cute son, Jun.

REFERENCES

Ahangar, F.A., 2012: Feasibility study of developing a binary power plant in the low-temperature geothermal field in Puga, Jammu and Kashmir, India. Report 6 in: *Geothermal training in Iceland 2012.* UNU-GTP, Iceland, 1-26.

Bejan, A., and Moran, M., 1996: *Thermal design and optimization*. John Wiley & Sons, Inc., NY, 533 pp.

Bertani, R., 2010: Geothermal power plants in the world 2005-2010 update report. *Proceedings of the World Geothermal Congress 2010, Bali, Indonesia*, 41 pp.

Dagdas, A., Ozturk, R., and Bekdemir, S., 2005: *Thermodynamic evaluation of Denizli Kizildere geothermal power plant and its performance improvement*. Energy Conversion and Management 46, 245–256.

Dipippo, R., 2008: *Geothermal power plants. Principles, applications, case studies and environmental impact*. Elsevier Ltd., Kidlington, UK, 493 pp.

Dorj, P., 2005: *Thermoeconomic analysis of a new geothermal utilization CHP plant in Tsetserleg, Mongolia.* University of Iceland, MSc thesis, UNU-GTP, Iceland, report 2, 74 pp.

Estévez S., J.R., 2012: *Geothermal power plant projects in Central America: technical and financial feasibility assessment model.* University of Iceland, MSc thesis, UNU-GTP, Iceland, report 4, 87 pp.

Franco, A., and Villani, M., 2009: Optimal design of binary cycle power plants for water-dominated, medium-temperature geothermal fields. *Geothermics, 38-4,* 379-391.

Jalilinasrabady, S., Itoi, R., Valdimarsson, P., Saevarsdóttir, G., Fujii, H., 2012: Flash cycle optimization of Sabalan geothermal power plant employing exergy concept. *Geothermics, 43,* 75-82.

Lin W.J., and Liu Z.M., 2013: *Geothermal resource distribution and capacity estimation in China* (in Chinese). China Geology, 10 pp.

Rosyid, H., Koestoer, R., Putra, N., Nasruddin Mohamad, A.A., and Yanuar, 2010: Sensitivity analysis of steam power plant-binary cycle. *Energy, 35-9,* 3578-3586.

Sun C.X., 2008: *Feasibility study of geothermal utilization of Yangbajain field in Tibet autonomous region, P.R. China.* University of Iceland, MSc thesis, UNU-GTP, Iceland, report 3, 85 pp.

Valdimarsson, P., 2011: Basic concepts of thermoeconomics. *Presented at "Short Course on Geothermal Drilling, Resource Development and Power Plants", UNU-GTP and LaGeo, San Salvador, El Salvador,* 7 pp.

Valdimarsson, P., 2014: *Thermodynamics of geothermal power production*. UNU-GTP, Iceland, unpubl. lecture notes.

Wang J.Y., Ma W.B., 2005: *Geothermal utilization* (in Chinese*).* Chemical Industry Press, 147 pp.